Formaldehyde in the Alaskan Arctic snowpack: Partitioning and physical processes involved in air-snow exchanges

M. Barret, F. Domine, S. Houdier, J. C. Gallet, P. Weibring, J. Walega, A. Fried, D. Richter

Formaldehyde in the Alaskan Arctic snowpack: Partitioning and physical processes involved in air-snow exchanges

Manuel Barret,[1] Florent Domine,[1] Stephan Houdier,[1] Jean-Charles Gallet,[1] Petter Weibring,[2] James Walega,[2] Alan Fried,[2] and Dirk Richter[2]

Received 30 March 2011; revised 7 June 2011; accepted 14 June 2011; published 17 September 2011.

[1] The snowpack is a photochemically active medium which produces numerous key reactive species involved in the atmospheric chemistry of polar regions. Formaldehyde (HCHO) is one such reactive species produced in the snow, and which can be released to the atmospheric boundary layer. Based on atmospheric and snow measurements, this study investigates the physical processes involved in the HCHO air-snow exchanges observed during the OASIS 2009 field campaign at Barrow, Alaska. HCHO concentration changes in a fresh diamond dust layer are quantitatively explained by the equilibration of a solid solution of HCHO in ice, through solid-state diffusion of HCHO within snow crystals. Because diffusion of HCHO in ice is slow, the size of snow crystals is a major variable in the kinetics of exchange and the knowledge of the snow specific surface area is therefore crucial. Air-snow exchanges of HCHO can thus be explained without having to consider processes taking place in the quasi-liquid layer present at the surface of ice crystals. A flux of HCHO to the atmosphere was observed simultaneously with an increase of HCHO concentration in snow, indicating photochemical production in surface snow. This study also suggests that the difference in bromine chemistry between Alert (Canadian Arctic) and Barrow leads to different snow composition and post-deposition evolutions. The highly active bromine chemistry at Barrow probably leads to low HCHO concentrations at the altitude where diamond dust formed. Precipitated diamond dust was subsequently undersaturated with respect to thermodynamic equilibrium, which contrasts to what was observed elsewhere in previous studies.

Citation: Barret, M., F. Domine, S. Houdier, J.-C. Gallet, P. Weibring, J. Walega, A. Fried, and D. Richter (2011), Formaldehyde in the Alaskan Arctic snowpack: Partitioning and physical processes involved in air-snow exchanges, *J. Geophys. Res.*, *116*, D00R03, doi:10.1029/2011JD016038.

1. Introduction

[2] The snowpack is a complex multiphase photochemical reactor known to exchange reactive species with the atmosphere [*Anastasio and Robles*, 2007; *Beine et al.*, 2008; *Domine and Shepson*, 2002]. Formaldehyde (HCHO) is one of these noteworthy species. HCHO is not only the most abundant carbonyl compound in the atmosphere but, above all, a key reactive trace gas which significantly contributes to the oxidizing capacity of the atmosphere, especially in polar regions [*Chen et al.*, 2007]. Indeed, HCHO is formed by the oxidation of atmospheric organic gases but it is also, through its photolysis, a precursor of HO_x radicals [*Hutterli et al.*, 1999; *Perrier et al.*, 2002; *Sumner and Shepson*, 1999]. Both the production of HCHO in the snowpack and its release to the atmosphere, as well as the uptake of HCHO by the snow from the atmosphere may involve several processes.

[3] It is likely that HCHO can be produced via direct photolysis of light-absorbing organic compounds located in snow, and via oxidation of these organics by photo-formed oxidants such as hydroxyl radicals produced, for instance, by the photolysis of hydrogen peroxide in snow [*Anastasio and Robles*, 2007; *Anastasio et al.*, 2007; *Grannas et al.*, 2007]. However, the nature of organic chromophores in surface snow layers remains largely unknown, which makes it impossible to predict quantitatively HCHO production by photochemical processes.

[4] Exchanges of HCHO between the atmosphere and the snow through physical processes are also possible. Because HCHO is highly soluble in water [*Barret et al.*, 2011; *Betterton and Hoffmann*, 1988], water droplets efficiently scavenge atmospheric HCHO [*Ervens et al.*, 2003; *Matsumoto et al.*, 2005]. However, in general, species are much less soluble in ice than in water [*Thibert and Domine*, 1997, 1998], and initial studies of HCHO air-snow exchange [*Hutterli et al.*, 1999, 2002] proposed an empirical law to describe the observed partitioning of HCHO between snow and atmosphere. The

[1] Laboratoire de Glaciologie et Géophysique de l'Environnement, CNRS and Université Joseph Fourier – Grenoble I, Saint-Martin-d'Hères, France.
[2] Earth Observing Laboratory, National Center for Atmospheric Research, Boulder, Colorado, USA.

0148-0227/11/2011JD016038

partitioning law proposed in such studies was not backed up by robust studies of the HCHO adsorption and diffusion into ice, so that their sorption parameters may not actually correspond to thermodynamic parameters. Since then, subsequent studies have established that HCHO forms a solid solution with ice [*Barret et al.*, 2011; *Burkhart et al.*, 2002; *Perrier et al.*, 2003; *Perrier et al.*, 2002] and *Barret et al.* [2011] explained HCHO air-snow exchanges at Alert (Canadian high Arctic) by solid state diffusion of HCHO dissolved into the ice crystalline lattice of snow crystals. The solubility of HCHO in ice is sufficient for the snow to constitute a major HCHO reservoir. *Perrier et al.* [2002] calculated that, at Alert, at least 80% of the total amount of HCHO present in the system comprised of the atmospheric boundary layer and of the snowpack is found in snow. Therefore, the potential impact of the snowpack on HCHO atmospheric concentration is high.

[5] The main difficulty in understanding and quantifying snowpack HCHO emissions lies in the fact that both photochemical production and physical exchange are likely to emit HCHO to the atmosphere. In most studies reporting HCHO snowpack emissions [*Hutterli et al.*, 1999; *Perrier et al.*, 2002; *Sumner and Shepson*, 1999; *Sumner et al.*, 2002], the lack of thermodynamic data on the physical exchanges of HCHO makes it difficult to interpret the measured fluxes between the snowpack and the atmosphere and to quantify the contribution of both photochemical and physical processes.

[6] We propose here to investigate the physical processes involved in air-snow exchanges of HCHO. Recent data on the thermodynamics of the HCHO solid solution in ice [*Barret et al.*, 2011] and on the adsorption of HCHO on ice surfaces [*Collignon and Picaud*, 2004; *Hantal et al.*, 2007; *Winkler et al.*, 2002] allow detailed tests of the potential incorporation and exchange mechanisms. In particular, it is now possible, given the partial pressure of HCHO, P_{HCHO}, and the temperature T, to quantify the amount of HCHO adsorbed at the surface of snow crystals and the amount dissolved in the bulk of ice at thermodynamic equilibrium. Knowing the relative contribution of both these processes is essential because adsorbed molecules are exchanged on a very short timescale whereas HCHO dissolved into ice crystals has to diffuse through the ice crystalline lattice before being emitted to the gas phase.

[7] With this aim, we performed the simultaneous measurements of HCHO in the snow and in the atmosphere during the OASIS 2009 field campaign that took place in Barrow, Alaska. This study reports HCHO concentrations in the Barrow snowpack from March to April 2009, with a close focus on the very surface snow layers. These surface layers mostly consisted of diamond dust (DD), i.e. clear sky precipitation usually composed of small columns and bullet rosettes, which formed snow layers a few mm thick [*Walden et al.*, 2003]. Since the interpretation of fluxes between the snow and the atmosphere requires the knowledge of snow physical properties [*Domine et al.*, 2008], they were also monitored, especially the snow specific surface area (SSA) which quantifies the surface area of the ice-air interface at the crystal scale [*Domine et al.*, 2007; *Legagneux et al.*, 2002]. In this work, we elaborated a numerical model which uses the thermodynamics of HCHO-ice solid solutions, environmental variables such as P_{HCHO} and the snow physical parameters (SSA and temperature), to compute HCHO diffusion into ice crystals. These calculations allowed us to better understand the role of some processes involved in the post deposition evolution of HCHO concentration in snow. Our findings are also of interest for modeling post deposition processes that affect snow and ultimately firn concentrations and may therefore help to invert ice core data to reconstruct past HCHO atmospheric concentrations [*Hutterli et al.*, 2002].

2. Methods

2.1. Snow Sampling

[8] Snow samples were collected in 60 mL borosilicate glass vials for EPA analysis (Kimble Glass Inc., Vineland, NJ) with PTFE/silicone-lined caps. Vials were washed with ultrapure water and carefully rinsed just before sampling. Vials were equilibrated to ambient temperature and filled with snow by inserting them horizontally in the layer of interest. For DD samples, snow was collected by carefully scraping the surface layer with the vial. Drifting snow was collected in small pits dug specifically to trap that snow, which were sampled once sufficient amounts of snow had accumulated in them. Depending on snow density, the water-equivalent volumes collected ranged from 5 to 20 mL. After collection, samples were stored at −40°C and thawed just before chemical analysis. Blanks made of ultrapure water were stored in 60 mL vials at −40°C. They were analyzed for HCHO regularly and no contamination was detectable during storage. Polyethylene gloves were used for vial preparation and sampling to prevent contamination.

2.2. Chemical Analysis

[9] The analytical procedure followed is described by *Houdier et al.* [2000] with subsequent improvements detailed by *Houdier et al.* [2011]. Briefly, HCHO was analyzed by using DNSAOA derivatization followed by HPLC separation and fluorescence detection. Formaldehyde concentrations in the snow, [HCHO], are reported in parts per billion by weight, ppbw (1 ppbw = 1 μg L^{-1}). The detection limit is below 0.3 ppbw with overall accuracy better than 5%.

2.3. Gas Phase Measurements

[10] Measurements of gas-phase HCHO were acquired with a Difference Frequency Generation Absorption Spectrometer (DFGAS), which is described in detail by *Weibring et al.* [2007, 2010]. This instrument was modified to simultaneously acquire measurements of methane with HCHO. Briefly, ambient air was drawn continuously at a minimum of 10 sLpm through three heated (35°C) 1/2″ OD electropolished stainless steel tubes extending to various heights (~0.6 m, 1.5 m, and 5.4 m off the snow) on a sampling tower. The flow would increase, as each instrument connected to the tubes would cycle independently to sample from the tubes. When sampling, the DFGAS instrument draws an additional 9 sLpm and the TOGA instrument (Trace Organic Gas Analyzer, see *Apel et al.* [2003] for more details) draws an additional 5 sLpm. Each sampling line was tested for HCHO transmission efficiency by adding calibration standards to the entrance of each sampling inlet, and in all cases the retrieved HCHO was within 3% of the input values. Ambient air was sequentially sampled from the three tower heights into a

multipass absorption cell (effective path length of 100 m) controlled at 50 Torr pressure and temperatures ~24°C. Absorption data from a given sampling height was averaged for 30 s in 1-s increments and this was followed by a 10-s flush with zero air (supplied from a commercial Aadco zero air generator which quantitatively removes HCHO) before a 15-s averaged background spectrum was acquired. This background acquisition effectively removes optical noise as well as potential cell and line outgassing effects. Ambient air from the next sampling height flushed the system for 10 s before the acquisition of a new 30-s ambient average. The entire sequence was repeated. The time duration between the start of each new sampling height was ~65 s.

[11] Infrared light at 2831.6 cm^{-1} (3.53 μm), generated by mixing two near-IR room temperature lasers (one at 1562 nm and the other at 1083 nm) in a nonlinear crystal, was directed through the multipass absorption cell where the absorption due to a moderately strong and isolated vibrational-rotational transition of HCHO was detected. The absorption feature employed is free of all known spectroscopic interferences with the exception of weak methanol absorption features. These features produce a slight positive interference ranging between 0.3% and 2% for equivalent HCHO and methanol mixing ratios. Even though the methanol interference was not removed from the present measurements, on average its effect on the retrieved HCHO is insignificant. The average methanol-mixing ratio (3245 samples) by the TOGA instrument sampling through the same inlet over the course of this mission was 730 pptv, and this translates to an average HCHO error of only 2–15 pptv. The 15-s averaged background spectrum surrounding each ambient block was subtracted point-by-point from each 1-s ambient spectrum to arrive at a background-corrected ambient spectrum, which was then fit to a background-corrected reference spectrum, obtained by introducing a high concentration calibration standard (12 to 14 ppbv range) into the instrument inlet as needed. Calibrations standards in zero air were also periodically introduced into the system and treated like an ambient measurement to check the calibration stability and system drifts. The limit of detection (LOD at 1σ) was estimated for each 30-s ambient measurement block to be 30 pptv with an estimated systematic uncertainty of 6.9% (1σ) times the ambient mixing ratio.

[12] Because contamination was possible from local installations, we defined a clean air sector. Basically, "clean" days correspond to wind direction coming from the 0–110° sector. More details on pollution episodes and relation between meteorological conditions and HCHO mixing ratios are given by A. Fried (unpublished data, 2009). Elevated spikes of P_{HCHO} such as those observed during 21 March (Figure 3) are likely due to pollution plumes originating from local installations (A. Fried, unpublished data, 2009).

2.4. Solid State Diffusion Numerical Code

[13] A numerical code was developed to compute the variations of the HCHO concentration in snow caused by variations of P_{HCHO}, assuming that HCHO equilibrium in snow crystals is reached by solid state diffusion in the ice crystalline lattice. This model was applied to the top surface layer of freshly deposited diamond dust to compute the post depositional evolution of this layer at the interface between the snowpack and the atmosphere. Because the diffusion of HCHO in ice is order of magnitude lower than diffusion of HCHO in the gas phase [*Barret et al.*, 2011], we neglected the gas phase diffusion. The model is based on a Crank-Nicolson scheme [*Crank and Nicolson*, 1996] with a time step of 10 min. The snow crystal is idealized as a sphere of radius R_{eq} which depends on the snow specific surface area (SSA), divided in concentric layers with a radius step of 50 nm. SSA (in $m^2\ kg^{-1}$) is the surface area of snow crystals accessible to gases per unit mass [*Legagneux et al.*, 2002] and thus affects the rate of exchange of gases with the atmosphere. For practical purposes, we assimilate snow crystals to ice spheres whose equivalent radius is $R_{eq} = 3/(\rho_{ice}\ SSA)$ so that our idealized snow crystals have the same surface area to bulk volume ratio as the real snow. The SSA of the diamond dust layer was measured by infrared reflectance at 1310 nm using the DUFISSS instrument which provides a fast and accurate measurement [*Gallet et al.*, 2009].

[14] At each time step, the boundary condition is obtained by assuming that the outer layer of the spherical crystal which is in contact with the atmosphere is at thermodynamic equilibrium with P_{HCHO} and T. HCHO is then allowed to diffuse in the ice lattice according to the diffusion equation:

$$\frac{\partial U}{\partial t} = D\left(\frac{\partial^2 U}{\partial r^2}\right) \tag{1}$$

In equation (1), $U = [HCHO] \times r$, where r is the distance from the center of the sphere and varies between 0 and R_{eq}, D is the diffusion coefficient of HCHO in ice for which we used the value $D_{HCHO} = 6\ 10^{-12}\ cm^2\ s^{-1}$ as recommended by *Barret et al.* [2011] for temperatures comprised between 243 and 266 K. This common change of variable makes the calculations easier for diffusion problems in spherical media [*Carslaw and Jaeger*, 1959].

[15] The convergence of our model has been compared to the analytical solution of the following diffusion problem [*Carslaw and Jaeger*, 1959] (i) initial concentration in the sphere is null and (ii) for time $t > 0$, the concentration at the surface of the sphere remains equal to unity. Due to the jump discontinuity in the initial condition, the Crank-Nicolson scheme responds with undesired oscillations. These oscillations have been damped by solving the first iteration with an implicit method which does not affect the final convergence [*Østerby*, 2003]. Our computed solution was in excellent agreement both in time and in space with the analytical solution for a spatial resolution of 50 nm and a time step of 10 min, which are the parameters that were subsequently used. The damping method was applied every 10 time steps in our case study to prevent oscillations generated by the fast variations of the boundary conditions caused by strong P_{HCHO} variations.

3. Results

3.1. Snow Stratigraphy

[16] The characteristics of the snowpack, including stratigraphies and physical properties of snow, are detailed by F. Domine et al. (Structure, specific surface area and thermal conductivity of the snowpack around Barrow,

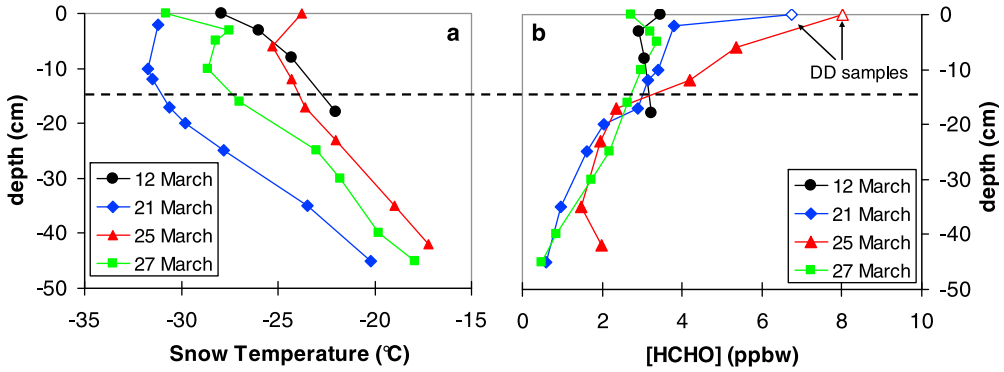

Figure 1. (a) Temperature and (b) [HCHO] profiles in different pits of similar stratigraphies between 12 and 27 March. The dotted line represents the boundary between the top wind-drift and the lower layers. Open symbols correspond to data for diamond dust (DD) samples.

Alaska, submitted to *Journal of Geophysical Research*, 2011a). Therefore only a brief summary of aspects relevant to our study are given below.

[17] The snow stratigraphy at Barrow was complex with multiple discontinuous layers and a high spatial variability at a meter scale. This type of snowpack, typical of the Arctic [*Domine et al.*, 2002], results from small amounts of precipitation associated with strong snow remobilization during wind episodes. During these episodes, the formation of new wind-drifts and the erosion of surface layers made it impossible to monitor a single snow layer during the whole campaign.

[18] The lowermost layer of the snowpack consisted of approximately 10–25 cm of depth hoar with sometimes columnar depth hoar close to the ground. Over the depth hoar was typically a 10–20 cm thick hard wind-packed layer, sometimes interrupted by a discontinuous layer of faceted crystals or by a melt-freeze crust. During wind episodes, the newly formed wind-drifts covered only a fraction of the ground surface, typically 20%, and could be up to 40 cm thick. In places, the wind-packed layer may be covered by a recent wind-drift to reach a height up to 70 cm above the ground. The mean thickness of the snowpack was 41 cm but strong spatial variations were observed. At the beginning of the campaign, a melt-freeze crust a few mm thick covered about 50% of the surface. From mid March, several DD falls were observed during clear days, forming a layer a few mm thick that could easily be sampled over the melt-freeze crust. DD has typically SSA in the 80–100 m^2 kg^{-1} range (F. Domine et al., The specific surface area and chemical composition of diamond dust near Barrow, Alaska, submitted to *Journal of Geophysical Research*, 2011b).

3.2. Vertical Profiles of HCHO

[19] Several snow pits were dug during the campaign to obtain vertical profiles of HCHO. In Figure 1 we report [HCHO] in 4 snow pits dug in March. The snow pits of 12, 21 and 25 March were dug in the snowfield near the BARC building (N 71°19.395′; W 156°39.685′) whereas on 27 March the snow pit was dug 8 miles south of Point Barrow (N 71°18.098′; E 156°46.070).

[20] A strong wind episode occurred on 9–12 March and formed several wind-drifts over the sampling area. The stratigraphies of pits dug from 12 to 25 March were similar, and the top 15 cm of the snowpack could easily be identified as the wind-drifted snow layer deposited on 9–12 March. Under this recent layer were older wind-packed layers and depth hoar. DD precipitated during clear days at the top of the snowpack to form a very uncohesive layer a few mm thick which was sampled separately (Domine et al., submitted manuscript, 2011b). On 26 March, a wind storm without any precipitation remobilized the entire DD layer, but also the wind-drifted layers formed on 9–12 March. On 27 March, after the storm, no distinguishable diamond dust layer was observed and the pit was dug at a location where a 15 cm thick new wind-drift formed, so that the comparison between all these pits is possible because of the similar stratigraphy in the surface layers.

[21] In all pits, temperature increased with depth (Figure 1a), while SSA decreased (Domine et al., submitted manuscript, 2011a). The main [HCHO] trend is a decrease with depth, although in fresh wind drifts studied, [HCHO] is almost homogeneous (12 and 27 March). The 12 March profile however indicates a slight increase of [HCHO] from 2.9 to 3.2 ppbw between −3 and −18 cm which is probably due to a higher sublimation of snow crystals by wind in the surface snow layers (see discussion in 4.4.1). Deep layers made of depth hoar showed almost no time variations between the start and the end of the campaign. The observed variability at the bottom of pits can be explained by spatial heterogeneity and contamination by vegetation. When comparing [HCHO] profiles obtained between 12 March and 25 March, which was a sunny period with light to zero wind, we observed that [HCHO] increased from 3.2 to 5.4 ppbw in the top wind-drift, while [HCHO] reached 8 ppbw in diamond dust. The vertical and temporal [HCHO] gradients visible in Figure 1b suggest a continuous uptake of HCHO from 12 to 25 March in the first 15 cm of the snowpack. After the windstorm which took place on 26 March, the profile obtained on 27 March showed concentrations similar to those observed on 12 March with no strong vertical gradient, suggesting mixing caused by wind, and a loss of HCHO during wind drifting.

[22] Since the time variations of [HCHO] were maximal in the uppermost layers of the snowpack, a specific effort was made to monitor [HCHO] in DD with a sufficient time resolution to detect diurnal variations.

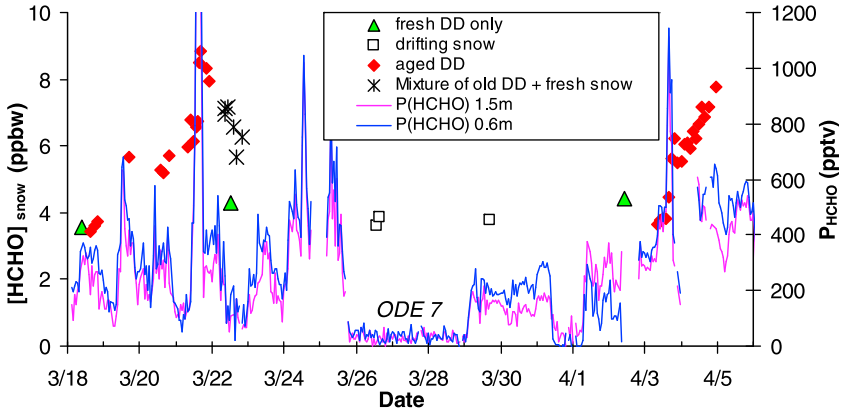

Figure 2. Temporal evolution of [HCHO] in the diamond dust layers and in drifting snow. Data for drifting snow and fresh diamond dust are differentiated from the aging DD layer. P_{HCHO} at 1.5 and 0.6 m are also reported by solid lines.

3.3. Time Evolution of [HCHO] in the Diamond Dust Layer

[23] Diamond dust precipitations were observed on 14–18, 22 March and 1–3 April (Domine et al., submitted manuscript, 2011b). These few millimeter-thick DD layers at the top of the snowpack subsequently metamorphosed until a new wind episode remobilized them. Because DD layers were very light and deposited over the harder wind-packed layer or the melt-freeze crust, DD was easy to collect for chemical analysis without sampling the underlying snow. On 22 March, snow fell in the morning while the layer deposited on 18 March was still on the ground. In the afternoon, the weather became clear and new DD fell. In order to sample only the fresh precipitating DD, we had previously swept clean an area on the melt-freeze crust.

[24] Figure 2 reports the time-evolution of [HCHO] in DD layers for the 18 March to 5 April period. For a better understanding, freshly fallen DD (less than 5 h old) is differentiated from the aging DD, and from the snow that fell on 22 March. [HCHO] measured in drifting snow during wind episodes is also reported. [HCHO] in DD ranged from 3.4 to 8.9 ppbw. [HCHO] in drifting snow and in fresh diamond dust were among the lowest values measured and ranged from 3.0 to 4.4 ppbw. The highest values were found in aged diamond layers during high P_{HCHO} episodes observed on 21, 26 March and 3–4 April. The low P_{HCHO} measured during 26–29 March are concomitant with an ozone depletion event (ODE), a phenomenon typical of the polar marine environment (see discussion below).

[25] Since we suspected that [HCHO] in diamond dust may reflect P_{HCHO} variations, we performed an intensive sampling campaign after a new diamond dust layer deposited on 2 April. From 3 to 5 April, the DD layer was sampled every 2 h, revealing an essentially continuous increase in [HCHO].

[26] As shown in Figure 2, P_{HCHO} reached extremely low values around 50 pptv during the 26–29 March period. This is concomitant with the longest ozone depletion event (ODE) which occurred during the campaign, called ODE 7. ODEs involve bromine chemistry that catalytically destroy ozone via reactions (2) and (3) [*Barrie et al.*, 1988]. However, HCHO can also react with Br [*Grannas et al.*, 2002; *Sumner and Shepson*, 1999], which competes with the ozone destruction process while consuming atmospheric HCHO (4):

$$Br + O_3 \rightarrow BrO + O_2 \quad (2)$$

$$2\ BrO \rightarrow 2\ Br + O_2 \quad (3)$$

$$HCHO + Br \rightarrow HBr + HCO \quad (4)$$

The low values of P_{HCHO} around 40 pptv during ODE 7 are consistent with what is expected when ozone is completely depleted [*Shepson et al.*, 1996; *Sumner and Shepson*, 1999]. However, since snow can also exchange HCHO with the atmospheric boundary layer, it is crucial to quantify how such a dramatic P_{HCHO} variation can impact [HCHO] in the snowpack.

4. Discussion

4.1. Snow/Atmosphere Partitioning of HCHO

[27] Our data show that [HCHO] can increase from 1 ppbw in the deepest layers to more than 8 ppbw in diamond dust. Using the density, thickness and mean [HCHO] of snow layers, we calculated the mean HCHO mass in the snowpack per unit surface area. The HCHO loading of the snowpack was calculated for several snow pits but we only report here (Table 1) the results for the two pits which showed the minimal (4 March) and maximal (25 March) HCHO loading in the continental snowpack.

[28] The difference between both dates is the height and the age of the top layers. The pits presented in Table 1 were dug 30 m apart, revealing the spatiotemporal variability of snowpack stratigraphy. On 4 March, 7 cm of fresh wind-drifted snow were overlying 26 cm of depth hoar and the typical old wind-packed layer was absent, probably eroded by wind at the sampling site. On 25 March, we also observed a 7 cm-thick layer of wind-drifted snow that accumulated during the 9–12 March storm. By 25 March, the clear meteorological conditions and the very low wind speeds allowed this wind-drifted layer to metamorphose into

Table 1. Total HCHO Mass per Unit Surface in the Snowpack, 2 Days After a Strong Windstorm (4 March), and After 12 Days With No Wind and Sunny Weather (25 March)

	Thickness (cm)	Density (kg m^{-3})	$[HCHO]_{snow}$ (ppbw)	HCHO Loading (ng cm^{-2})	Contribution (%)
4 March					
wind-drifted snow	7	384	2.8	7.3	36.1
depth hoar	4	145	2.2	1.3	6.4
indurated depth hoar	5	370	1.8	3.2	16.0
depth hoar	3	220	1.9	1.2	6.1
columnar depth hoar	14	276	2.0	7.2	35.5
Total	33			20.3	100
25 March					
diamond dust	0.5	165	8.0	0.7	1.6
faceted wind-drifted snow	7	303	5.4	11.4	28.0
wind-packed snow	13	351	3.3	14.9	36.7
depth hoar	27	250	2.2	13.7	33.6
Total	47.5			40.6	100

faceted crystals. As previously shown in Figure 1, an increase of [HCHO] in this layer was also observed.

[29] The total loading of the snowpack varied from 20.3 to 40.6 ng cm^{-2} between these two typical snowpacks, and the contribution of each snow layers is detailed in Table 1. It is noteworthy that the total HCHO loading of depth hoar layers is almost the same with values around 13 ng cm^{-2} and that the difference in the HCHO loading is essentially due to the variable contribution of the top layers. On 25 March, the top layers (diamond dust + faceted wind-drift + wind-packed snow) contribution accounts for 27 ng cm^{-2} whereas on 4 March, the top layer only accounts for 7 ng cm^{-2}, yielding a twice as high HCHO loading on 25 March. This difference in the HCHO loading of the snowpack is due to both the spatial variability in the thickness of the top layers and to the time variations of [HCHO] in the surface layers. Although [HCHO] in DD layers can reach values as high as 8.9 ppbw (Figure 2), these thin and light layers do not contribute significantly to the total loading of the snowpack (1.6%) because of their small mass per surface area.

[30] Knowing the amount of HCHO in the snowpack, we can calculate the partitioning of HCHO between the snow and the atmospheric boundary layer, using, as key variables, P_{HCHO} and the height of the mixing layer. This latter variable was estimated to be 200 m during calm and sunny conditions, whereas during wind storms it could reach 1200 m (R. Staebler, personal communication, 2011). Between 18 March and 14 April, the mean P_{HCHO} measured at a height of 5.4 m was 204 pptv, and in the absence of vertical profiles at higher altitudes, we assumed that P_{HCHO} was homogeneous within the 200 m mixing layer. As a result, we calculated that 80% to 89% of the total HCHO (in the atmosphere and in the snowpack) was located in the snow, depending on the loading of the snowpack. The snowpack therefore does act as an important HCHO reservoir. Windstorms remobilize the top layers, which contribute to 34–76% of the total snowpack loading. Since wind remobilization results in snow sublimation, the potential release of HCHO from these layers during windstorms is high.

4.2. Incorporation Processes of HCHO in Snow

[31] Understanding quantitatively the mechanism of incorporation of gases in ice has often been only partially successful [*Domine and Thibert*, 1996; *Domine et al.*, 1995; *Hutterli et al.*, 1999, 2002; *Perrier et al.*, 2002] because crucial data on the relevant processes was lacking. However, recent experimental results [*Barret et al.*, 2011; *Hantal et al.*, 2007; *Winkler et al.*, 2002] make such an attempt worthwhile here.

[32] The possible incorporation processes of HCHO in snow are (i) adsorption onto the surface of crystals, (ii) formation of a solid solution and equilibration by solid-state diffusion and (iii) dissolution into organic aerosols trapped in the snow. This latter hypothesis will not be discussed here, because the exact nature of the aerosols involved is unknown and this makes it difficult to estimate the solubility of HCHO in particulate matter. However, it was shown that, in suburban environments, HCHO associated to the particle phase was negligible [*Odabasi and Seyfioglu*, 2005].

4.2.1. Adsorption Onto the Surface of Ice Crystal

[33] According to the experimental study of *Winkler et al.* [2002], adsorption of HCHO on ice between 198 and 223 K follows a Langmuir isotherm. However, their results cannot be extrapolated to higher temperatures because they could not calculate the adsorption enthalpy (ΔH_{ads}) of HCHO on ice. In a recent numerical study, *Hantal et al.* [2007] calculated the adsorption isotherm and ΔH_{ads} of HCHO on ice at 200 K. They also found that HCHO adsorbed weakly to ice surfaces with $\Delta H_{ads} = -27.3$ kJ mol^{-1}. These two studies allow us to calculate an upper limit for the amount of adsorbed molecules on snow crystals at Barrow. Using the most favorable conditions for adsorption that were encountered during the campaign, i.e., SSA = 85 m^2 kg^{-1}, P_{HCHO} = 1000 pptv and temperature T = 233 K, we found that the adsorbed fraction of HCHO only reaches 0.1 ppbw which is only 3% of the typical concentrations measured in snow. Adsorption of HCHO on snow crystals is therefore negligible.

4.2.2. Dissolution in the Volume of Ice Crystals

[34] The incorporation of HCHO in snow by the formation of a solid solution has been previously proposed to explain [HCHO] in snow [*Burkhart et al.*, 2002; *Perrier et al.*, 2003]. However, the data on HCHO solid solutions in ice and on the kinetics of equilibration were not sufficient to test this incorporation mechanism for natural snow. Indeed, experiments performed by *Burkhart et al.* did not allow snow to reach equilibrium, and *Perrier et al.* [2003] performed only two experiments at a single temperature

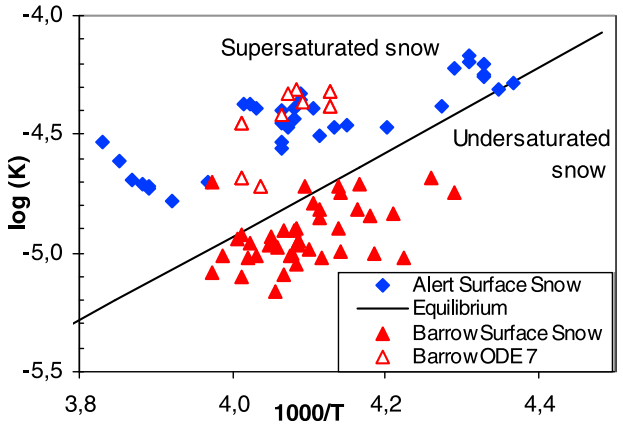

Figure 3. Arrhenius plot of the partitioning coefficient K(T) for surface snow layers. Data obtained during ODE 7 are also indicated as well as values calculated from the previous Alert field campaign in 2000 [*Perrier et al.*, 2002].

(−15°C), which makes the extrapolation to natural arctic snow uncertain. In a recent study, *Barret et al.* [2011] measured experimentally the solubility and the diffusivity of HCHO in ice over larger ranges of temperature (T = −7 to −30°C) and pressure (P_{HCHO} = 3.5 10^{-4} to 0.1 Pa). They found that HCHO diffuses very slowly into ice, with a diffusion coefficient D_{HCHO} = 6 10^{-12} cm^2 s^{-1} which suggests that several days to weeks are required for snow to equilibrate with the atmosphere. Their study of the thermodynamics of the HCHO-ice solid solution yields the following temperature and P_{HCHO} dependence of the HCHO molar fraction (X_{HCHO}) in ice:

$$X_{HCHO,\,ice} = 9.898 \times 10^{-13}\, e^{(4072/T)} (P_{HCHO})^{0.803} \qquad (5)$$

where P_{HCHO} is in Pa and T in K. Since the X_{HCHO} dependence on P_{HCHO} is not linear, the partitioning of HCHO between snow and atmosphere can be described by $K(T) = X_{HCHO} / P_{HCHO}^{0.803}$, K(T) following an Arrhenius law.

[35] We propose to test here whether the partitioning of HCHO observed during the campaign compares with this thermodynamic equilibrium. Because P_{HCHO} was not measured into the snow during the OASIS campaign, the equilibrium will be discussed only for surface snow layers (i.e. at depth less than 15 cm). Although the exact P_{HCHO} in the first 15 cm of the snowpack is not known, we will assume that P_{HCHO} can be approximated by P_{HCHO} measured 60 cm above the snow surface. In what follows, values of K(T) were calculated using the mean P_{HCHO} of the 24 h preceding the sampling date. The temperature to which this value is assigned is that of the snow layer at the time of sampling. This allows one to smooth potential daily cycles in P_{HCHO} at a timescale more consistent with the kinetics of diffusion. For a complete interpretation of [HCHO] in the whole snowpack, a snowpack model including heterogeneous chemistry associated with diffusion and advection of chemical species should be required, which is far beyond the objectives of this work. Figure 3 shows calculated values of K(T) for surface snow samples.

[36] Figure 3 shows that snow at Barrow was mainly undersaturated except during ODE 7 where snow was supersaturated with respect to the thermodynamic equilibrium. We attribute this apparent supersaturation to the very low P_{HCHO} (50 pptv) encountered during this ODE, which may be explained by bromine chemistry efficiently removing atmospheric HCHO [*Evans et al.*, 2003; *Shepson et al.*, 1996], while HCHO in snow remained around 2.7 to 4 ppbw (Figures 1 and 2).

[37] In Figure 3, we also reported the values calculated from data obtained during the Alert2000 field campaign which took place in the Canadian high arctic near Alert (Ellesmere Island 82.5°N, 62.3°W) in 2000. During that campaign both snow and atmospheric HCHO concentrations were measured and evidences for HCHO emission from fresh snow were observed [*Perrier et al.*, 2002; *Sumner et al.*, 2002]. *Perrier et al.* monitored [HCHO] in a fresh snowfall that occurred in April and observed that [HCHO] decreased to reach an apparent steady state value after a few days. From such an observation, it was suggested that HCHO in fresh snow was supersaturated at the time of precipitation, and subsequently emitted HCHO to the atmosphere, which was confirmed by HCHO flux measurements out of the snowpack reaching 2 10^9 molecules cm^{-2} s^{-1} on 18 April 2000 [*Grannas et al.*, 2002]. Our calculation of K(T) values for this data set confirms that snow at Alert was supersaturated with respect to the thermodynamic equilibrium of HCHO solid solution in ice.

[38] Since Alert and Barrow data are scattered around the thermodynamic equilibrium, dissolution of HCHO in ice and the formation of a solid solution appears to be the most likely incorporation process. However, further quantitative tests are needed to understand why snow is not at thermodynamic equilibrium.

4.3. Testing Solid State Diffusion as the Equilibration Process

[39] The main objective of the intensive sampling period from 3 to 5 April 2009 was to test whether solid state diffusion of HCHO into snow crystals could explain [HCHO] changes in snow. Ideally, data from this period could also have been used to quantify HCHO fluxes into the snow and to the atmosphere under typical polar conditions. Unfortunately, the wind direction was not optimal so that the air mass was probably contaminated by anthropogenic emissions. This is not an issue for the understanding of the physical processes involved in the exchange of HCHO between snow and atmosphere, but the calculation of HCHO fluxes that one could make during this period is not relevant to polar chemistry. We therefore do not perform such flux calculations, for which we chose a period with better wind directions, even though snow measurements were not done with as short a time step as in this case.

[40] As discussed above, the diamond dust layer was monitored regularly and showed a significant increase in [HCHO] while P_{HCHO} increased. When interpreting gas exchanges between snow and atmosphere, the knowledge of snow specific surface area (SSA) is required to quantify the gas fluxes through the surface of ice crystals and this variable was therefore monitored. The SSA of the studied DD layer showed small variations with a mean value of SSA = 80 m^2 kg^{-1} so that we calculated an equivalent radius for ice crystals of R_{eq} = 41 μm.

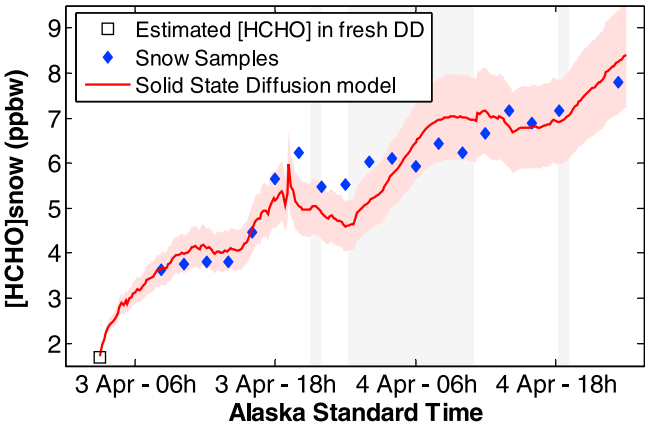

Figure 4. Computed and measured concentration in the diamond dust layer for 3 to 5 April. Grey zones indicate periods when P_{HCHO} was interpolated because no data was available. The red zone indicates calculations performed with ±15% error on the solubility of HCHO.

4.3.1. Computed Snow Concentrations

[41] Evolution of [HCHO] at the crystal scale was calculated using the numerical code presented in **2.4**. Our model needs to be initialized at the beginning of the simulation with an initial concentration within the grain. The formation of DD occurs by condensation of water vapor from the gas phase and it is difficult to predict the amount of HCHO incorporated from the gas phase into the growing ice crystals. Indeed, the incorporation of trace gases in ice grown from the gas phase requires the knowledge of several kinetics parameters such as the sticking coefficient of HCHO in ice and the growth rate of ice [*Domine and Thibert*, 1996; *Domine and Rauzy*, 2004]. Because data for these processes are not available, we will assume that the initial concentration of diamond dust, $[HCHO]_0$, is homogeneous within the grain and that $[HCHO]_0$ can differ from thermodynamic equilibrium. Once deposited onto the ground, diamond dust tends toward the thermodynamic equilibrium by solid-state diffusion of HCHO into the ice crystal.

[42] There was no automatic measurement of precipitation during the campaign. Snowfalls and DD precipitation were determined by observations, but these were not continuous. The time of formation of DD and its initial concentration are therefore treated as unknowns in our model. The fresh diamond dust layer we focus on was first observed in the morning of 3 April, which leads us to suppose that DD deposited between 21:00 (2 April) and 6:00 (3 April). We simulated diffusion of HCHO into the ice crystals based on measured P_{HCHO} values and found that $[HCHO]_0$ = 1.7 ppbw at 3:00 on 3 April gave the best results and, in particular, reproduced the 3.6 ppbw concentration measured at 8:00 on 3 April. This latter set of values makes sense since at 3:00 the air temperature was close to its daily minimal value (−31°C), which may enhance the condensation of water vapor and therefore favor the formation of diamond dust. Although the initial $[HCHO]_0$ of 1.7 ppbw may sound low, we believe that such a value is not unrealistic. Indeed, an ODE lasted from 31 March to 2 April and we can reasonably assume that active bromine chemistry occurred in the air mass where diamond dust formed. This assumption is supported by ionic analyses of DD which showed a large enrichment in Br relative to seawater composition (Domine et al., submitted manuscript, 2011b). As bromine chemistry is known to deplete atmospheric HCHO (see reaction (4)), such a phenomenon may have subsequently limited [HCHO] in the growing DD crystals.

[43] As shown in Figure 4, the calculated evolution of [HCHO] is in good agreement with field measurements. Although the maximum amplitude is slightly underestimated in our model, the global trend is well reproduced, especially the decrease observed during the night of 3–4 April. We also performed similar simulations in which snow crystals shapes were approximated by thin plates 27 μm thick so that they have the correct SSA. Such calculations led to a slightly faster equilibration of snow crystals. Their HCHO concentrations at the end of the simulation were only 16% higher than those performed with the spherical approximation. Given the large difference in shape between spheres and plates, we conclude that crystal shape has little effect on exchanges of reactive species by solid state diffusion. Future work using actual snow crystal shapes would nevertheless be of interest. We believe that this good agreement confirms our hypothesis that [HCHO] in snow is explained by the formation of a solid solution of HCHO in ice, and that changes in [HCHO] take place by solid state diffusion with a diffusion coefficient of 6 10^{-12} cm^2s^{-1}. Figure 3 shows that at Barrow, the ice crystals remain undersaturated relative to the predicted equilibrium, because HCHO does not have sufficient time to diffuse into the whole snow grain. This slow diffusion produces a concentration gradient between the interface and the center of ice crystals, and this gradient has implications worth discussing.

4.3.2. HCHO Radial Distribution Into Ice Crystals

[44] Diffusion of HCHO in ice being slow, exchanges between snow and atmosphere observed at an hourly or daily scale will only involve HCHO located in the first few μm below the ice-air interface. In order to estimate how this will impact the mean concentration, we need to calculate the normalized cumulative distribution function (CDF) of [HCHO]. Using R_{eq}, CDF(r) can be calculated according to equation (6) which represents the contribution to the mean grain concentration of HCHO contained between the center of the grain and a radius r:

$$CDF(r) = \frac{1}{[HCHO]} \int_{u=0}^{r} C(u)\ 4\ \pi\ u^2\ du \qquad (6)$$

where [HCHO] is the mean concentration of the ice crystal, C(u) is the HCHO concentration in the ice crystal at a distance u from the center.

[45] Using calculations done with our diffusion model, we calculated the CDF in ice crystals for the diamond dust fallen on 3 April 2009 at Barrow which subsequently took up HCHO from its initial concentration $[HCHO]_{0,\ Barrow}$ = 1.8 ppbw. For comparison the same calculations were performed for the 7S snow layer that deposited on 13–14 April 2000 at Alert and which released HCHO for several days [*Perrier et al.*, 2002]. Results of this calculation were previously shown by *Barret et al.* [2011] and we used the same initial homogeneous concentration $[HCHO]_{0,\ Alert}$ = 18 ppbw.

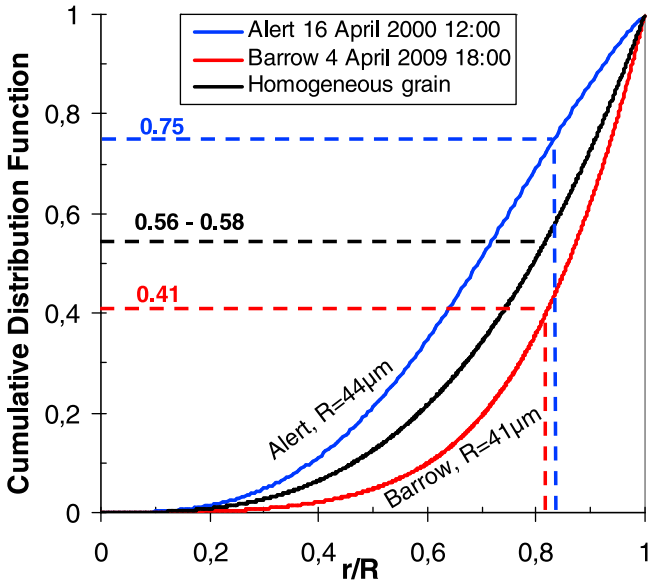

Figure 5. Cumulated Distribution Function of HCHO into ice crystals for fresh snow at Alert, diamond dust at Barrow and for a snow grain with a homogeneous [HCHO], as a function of relative radius r/R where R is the radius of the snow crystal. Dashed lines represent the relative contribution to the total [HCHO] of layers not affected by diffusion at the timescale of a day.

Both calculations were done for ice crystals 40 h after their deposition on the ground so that concentrations in snow evolved to $[HCHO]_{48h,\ Alert}$ = 9.8 ppbw and to $[HCHO]_{48h,\ Barrow}$ = 6.8 ppbw. Given the snow SSA of 80 and 75 $m^2\ kg^{-1}$ for the diamond dust layer at Barrow and the 7S layer at Alert, we found equivalent radii for ice spheres of R_{eq} = 41 and 44 μm, respectively. In Figure 5, we present these CDF and the amount of HCHO present in the outer volume of the snow crystals. On the time scale of 24 h, we can calculate the distance from the surface in which diffusion can significantly affect concentrations: $x_{diff} = \sqrt{D_{HCHO} \times t} = 7.2\ \mu$m. This indicates that diffusion will have almost no effect on [HCHO] from the center of the snow grain to 82–84% of R_{eq}.

[46] As shown in Figure 5, this inner region contains almost 75% of the total amount of HCHO in the snow of Alert, whereas for DD at Barrow it accounts for only 41%. This explains why [HCHO] at Alert was much less sensitive to changes in P_{HCHO} and T, since most of the HCHO was trapped into the core of ice crystals. On the contrary, the core of DD at Barrow contributed much less to the overall [HCHO], and the fast variations observed in [HCHO] can be explained by the concentration variations of the outer layers. This may also explain why the release of HCHO from wind-drifted snow was so efficient, as indicated in Figure 2. Indeed, drifting snow inevitably sublimates [*Domine et al.*, 2009; *Pomeroy and Li*, 2000; *Pomeroy et al.*, 1993], which affects the outer layers of snow grains, containing the major fraction of HCHO. To our knowledge, the only previous snow model that considered explicitly concentration gradients within ice crystals focused on H_2O_2 [*McConnell et al.*, 1998]. We believe that such an approach in a snow chemistry model would be useful to better understand HCHO fluxes to the atmosphere and [HCHO] measured in snow and thus to improve our understanding of ice core records [*Hutterli et al.*, 2003]. It is now possible to combine this understanding of the radial distribution with simultaneous snow and atmospheric measurements to constrain the HCHO budget and air-snow exchanges.

4.4. Applications

[47] Considering the equilibration of the solid solution of HCHO in ice by solid state diffusion as the mechanisms of incorporation of HCHO in snow crystals, and since we are aware that the [HCHO] within a snow grain is not homogeneous, we can try to explain some selected observations made during the OASIS campaign.

4.4.1. Release of HCHO to the Atmosphere During Wind Episodes

[48] During wind storms, wind-drifted snow grains were rounded by sublimation. As discussed above, the outer part of ice crystals, i.e., the part that sublimated, contained the major HCHO fraction, so that during sublimation the drifting snow is likely to release a significant amount of HCHO to the atmosphere. This is illustrated in what follows by studying the evolution of both the HCHO loading of the upper layers of the snowpack and the HCHO fluxes to the atmosphere during wind episodes.

[49] During the wind episode of 26 March, the wind coming from the clean air sector reached 7.5 m s^{-1} at 1 m above the ground. At the same time, the DD layer was blown off to form wind drifts, whose [HCHO] showed a significant decrease relative to the DD layer (Figure 1). Before the storm, on 25 March, the mean [HCHO] in the wind-drifted layer was 5.4 ppbw, whereas, after the storm, the mean [HCHO] in the fresh snow-drifts was 3.0 ppbw. It was not possible to monitor the chemical evolution of the snow-drifts during the storm. Therefore we made the hypothesis that, during the storm, snow was sufficiently remobilized and well mixed so that [HCHO] in fresh snowdrifts was spatially homogeneous. A drifting snow triplicate sample was nevertheless collected during the 26 March storm and [HCHO] snow concentration of 3.9 ppbw was measured. This is consistent with a decrease of snow concentrations from 5.4 before to 3.0 ppbw after the storm. From these observations, and assuming that HCHO lost from these particular surface snow layers was released to the atmosphere, we calculate that the mean HCHO flux emitted to the atmosphere and stemming from snow sublimation during this 24 h storm was 5.6 10^9 molecules $cm^{-2}\ s^{-1}$.

[50] In principle, such a flux should be detectable by gas phase HCHO measurements. However, once released from the snow, HCHO can be oxidized by OH or photolyzed, but also destroyed by Br chemistry (reaction (4)). On 26 March, a large ODE occurred, so that we can expect active bromine chemistry that explains the very low P_{HCHO} measured around 40 pptv. Because these values are very close to the detection limit, it was not possible to get an estimation of the atmospheric HCHO flux.

[51] However, on 31 March, wind speeds were also around 7.5 m s^{-1} and ozone was only partly depleted (9.3 ppbv), supporting a lesser active Br chemistry and explaining the higher P_{HCHO} (200 pptv). The strong vertical P_{HCHO} gradient during 31 March and the measurement of turbulent diffusivity makes it possible to calculate a HCHO flux of

$5.0 \pm 0.8\ 10^9$ molecules $cm^{-2}\ s^{-1}$ coming from the snow (A. Fried et al., unpublished data, 2009). This is consistent with an HCHO release from sublimating wind-blown snow crystals. Regular snow [HCHO] measurements for the 31 March period are not available.

[52] To evaluate the atmospheric importance of the HCHO emission from the snow on 26 March, we compared it to the flux of HCHO arising from the oxidation of methane (CH_4) by the OH radical, i.e. the main atmospheric source of HCHO. Assuming an average [OH] = $1\ 10^6$ molecules cm^{-3} (L. Mauldin, personal communication, 2011) and a rate coefficient k^+_{OHCH4} (245K) = $1.5\ 10^{-15}$ $molecules^{-1}$ $cm^3\ s^{-1}$, a production rate of $8.1\ 10^4$ molecules $cm^{-3}\ s^{-1}$ can be calculated. The release of HCHO by snow during the 26 March windstorm therefore equals the HCHO production by oxidation of CH_4 in a 690 m high air column. Since the height of the atmospheric mixing boundary layer ranged from 200 m to 1200 m, the release of HCHO by drifting snow may be a significant source of HCHO.

4.4.2. Possible Photochemical Production Into the Snowpack

[53] In what precedes, we showed that the variations of [HCHO] in the diamond dust layer are well reproduced by the equilibration of the HCHO-ice system by diffusion of HCHO in ice, the input parameters being the DD temperature and SSA, and P_{HCHO} at the snow/air interface. However, the source of HCHO was not identified and the high P_{HCHO} observed on 3–5 April may be related to air masses contaminated by anthropogenic emissions.

[54] To attempt to identify the HCHO source, we consider the time period of 18 to 19 March, when the wind direction was from the clean air sector, which should ensure that our data are free from local pollution. We observed a DD fall on 18 March morning, which formed a 5 mm-thick layer. [HCHO] increased from 3.7 ppbw (18 March, 20:25) to 5.4 ppbw (19 March, 16h30) which corresponds to an uptake of $2.6\ 10^{12}$ molecules cm^{-2}, i.e. a mean flux of $3.5\ 10^7$ molecules $cm^{-2}\ s^{-1}$. Data are insufficient to calculate the amount of HCHO incorporated in the lower layers, therefore the flux of HCHO into the snowpack has to be considered as a lower limit.

[55] At first glance we could suspect that the HCHO taken up by snow came from the atmosphere. However, the vertical gradient of P_{HCHO} demonstrates an upward flux of HCHO, showing that there is a source of HCHO within the snowpack. This emission may be due to photochemical production of HCHO in the upper layers of the snowpack and/or to the release of HCHO from deeper snow layers.

[56] Since depth hoar layers are warmer and contain less HCHO than recent snow layers, it could be suggested that they have been emitting HCHO. As detailed by Domine et al. (submitted manuscript, 2011a), no significant change in depth hoar physical properties was observed, and we did not observe any clear time-variation of [HCHO] in depth hoar layers during the campaign. This apparent steady state of hoar layers could indicate that those layers are at thermodynamic equilibrium, but in the absence of data for P_{HCHO} in the interstitial air, it is not possible to confirm this hypothesis. If we assume that the snow layers more than 20 cm deep are at thermodynamic equilibrium, we find that P_{HCHO} in interstitial air has to be in the 30–120 pptv range with the lowest values at the ground interface. Such values are lower than those usually measured above the snow (Figure 3) and would indicate that HCHO diffuses toward the lowermost layers of the snowpack, which is in contradiction with snowpack emissions from the basal layers. Physical emission from deep layers is therefore probably not important, and photochemical production appears the most likely source of the HCHO flux.

[57] Our preferred explanation is therefore that photochemical production occurred in the snowpack photic zone. HCHO produced in snowpack interstitial air subsequently both diffused to the atmosphere and into ice crystals of surface snow layers. The atmospheric flux during 18–19 March is estimated between 1 and 8×10^9 molecules $cm^{-2}\ s^{-1}$ (A. Fried et al., unpublished data, 2009) which is about 2 orders of magnitude higher than the flux incorporated into snow. That HCHO preferentially diffuses out to the atmosphere rather than incorporates into the snow is not surprising, given that HCHO has little affinity with ice surfaces [*Hantal et al.*, 2007; *Winkler et al.*, 2002]. It should not be concluded that the amount of HCHO incorporated in the snow is negligible. First, the atmospheric HCHO lifetime is only a few hours, whereas its observed stability in the snowpack (Figure 1) indicates that it is protected from photolysis when in solution within ice crystals. Whatever HCHO is incorporated into the snow can then affect the HCHO budget of the (snow + boundary layer) system for a long time. It can also be subsequently emitted to the atmosphere, for example when snow sublimates during windstorms.

[58] *Sumner and Shepson* [1999] hypothesized that HCHO was produced photochemically in the snowpack. Subsequent experiments performed at Alert showed that it is possible to photochemically produce HCHO and other carbonyl compounds in the snowpack from organic matter scavenged by snow [*Guimbaud et al.*, 2002; *Houdier et al.*, 2002; *Perrier et al.*, 2002; *Sumner et al.*, 2002]. Our results confirm that organic matter scavenged by snow is indeed the most likely source of HCHO coming out of the snow and incorporated into the snow crystals. As discussed by Domine et al. (submitted manuscript, 2011b) there are strong evidences that DD at Barrow had elevated organics concentrations and was involved in active photochemical reactions that are not only producing HCHO but also glyoxal and methylglyoxal. Presumably, these organics are in the form of aerosol particles which could originate from open leads in the sea ice off of Barrow.

5. Conclusion

[59] Measurements of HCHO both in the atmosphere and in the snowpack at Barrow during the OASIS field campaign allowed us to investigate the processes affecting exchanges of this gas between the snow and the atmosphere. We conclude that the variations of [HCHO] in snow can be quantitatively explained by considering the kinetics and thermodynamics of the solid solution of HCHO in ice. There is no need to invoke any processes taking place in the quasi-liquid layer that exists at the surface of ice crystals [*Cho et al.*, 2002; *Döppenschmidt and Butt*, 2000].

[60] The comparison of our data with those previously obtained at Alert indicates that the evolution of HCHO in the snowpack is influenced by the chemistry of halogens (and more specifically bromine) that took place at the time

and place where the snow formed. At Barrow, active bromine chemistry probably yielded low P_{HCHO} where snow formed in the free troposphere, leading to snow that was undersaturated with respect to conditions encountered at the ground level. The equilibration of precipitated snow with atmospheric P_{HCHO} is explained by kinetics and thermodynamics of HCHO solid solutions in ice, and requires the knowledge of the snow specific surface area. The fact that fluxes of HCHO were simultaneously observed both into snow and to the atmosphere indicates that photochemical production of HCHO took place in the snowpack photic zone, most likely in organic particles scavenged by the snow.

[61] We also made a reanalysis of HCHO data obtained during a previous polar campaign conducted at Alert. It appears that, at Alert, snow formed supersaturated in HCHO, and HCHO subsequently outgassed from snow on the ground. Even though gas phase measurements at Alert indicate that a photochemical production of HCHO probably exists, this production cannot be deduced from snow analyses which essentially revealed the degassing of HCHO. At Barrow, the important formation of first year sea ice associated to many open leads can explain the stronger halogen chemistry observed. This chemistry leads to completely different snow compositions and consequently to different post-deposition processes for HCHO exchanges with the atmosphere, which shed some new light on the physical processes involved in HCHO-snow interactions.

[62] **Acknowledgments.** The participation of M.B., F.D., S.H. and J.-C.G. to the Barrow field campaign was funded by the French Polar Institute (IPEV) grant 1017 to F.D. They also benefited from the general framework of the campaign provided by the U.S. National Science Foundation, and in particular they acknowledge efficient help and support by Harry Beine through grant NSF ATM-0807702. The National Center for Atmospheric Research is operated by the University Corporation for Atmospheric Research under the sponsorship of the National Science Foundation.

References

Anastasio, C., and T. Robles (2007), Light absorption by soluble chemical species in Arctic and Antarctic snow, *J. Geophys. Res.*, *112*, D24304, doi:10.1029/2007JD008695.

Anastasio, C., E. S. Galbavy, M. A. Hutterli, J. F. Burkhart, and D. K. Friel (2007), Photoformation of hydroxyl radical on snow grains at Summit, Greenland, *Atmos. Environ.*, *41*(24), 5110–5121, doi:10.1016/j.atmosenv.2006.12.011.

Apel, E. C., A. J. Hills, R. Lueb, S. Zindel, S. Eisele, and D. D. Riemer (2003), A fast-GC/MS system to measure C_2 to C_4 carbonyls and methanol aboard aircraft, *J. Geophys. Res.*, *108*(D20), 8794, doi:10.1029/2002JD003199.

Barret, M., S. Houdier, and F. Domine (2011), Thermodynamics of the formaldehyde-water and formaldehyde-ice systems for atmospheric applications, *J. Phys. Chem. A*, *115*(3), 307–317, doi:10.1021/jp108907u.

Barrie, L. A., J. W. Bottenheim, R. C. Schnell, P. J. Crutzen, and R. A. Rasmussen (1988), Ozone destruction and photochemical-reactions at polar sunrise in the lower arctic atmosphere, *Nature*, *334*(6178), 138–141, doi:10.1038/334138a0.

Beine, H., A. J. Colussi, A. Amoroso, G. Esposito, M. Montagnoli, and M. R. Hoffmann (2008), HONO emissions from snow surfaces, *Environ. Res. Lett.*, *3*(4), 045005, doi:10.1088/1748-9326/3/4/045005.

Betterton, E. A., and M. R. Hoffmann (1988), Henry's law constants of some environmentally important aldehydes, *Environ. Sci. Technol.*, *22*(12), 1415–1418, doi:10.1021/es00177a004.

Burkhart, J. F., M. A. Hutterli, and R. C. Bales (2002), Partitioning of formaldehyde between air and ice at −35°C to −5°C, *Atmos. Environ.*, *36*(13), 2157–2163, doi:10.1016/S1352-2310(02)00221-2.

Carslaw, H. S., and J. C. Jaeger (1959), *Conduction of Heat in Solids*, 2nd ed., Oxford Univ. Press, Oxford, U. K.

Chen, G., et al. (2007), An assessment of the polar HO_x photochemical budget based on 2003 Summit Greenland field observations, *Atmos. Environ.*, *41*(36), 7806–7820, doi:10.1016/j.atmosenv.2007.06.014.

Cho, H., P. B. Shepson, L. A. Barrie, J. P. Cowin, and R. Zaveri (2002), NMR investigation of the quasi-brine layer in ice/brine mixtures, *J. Phys. Chem. B*, *106*(43), 11,226–11,232, doi:10.1021/jp020449+.

Collignon, B., and S. Picaud (2004), Comparison between methanol and formaldehyde adsorption on ice: A molecular dynamics study, *Chem. Phys. Lett.*, *393*(4–6), 457–463, doi:10.1016/j.cplett.2004.06.085.

Crank, J., and P. Nicolson (1996), A practical method for numerical evaluation of solutions of partial differential equations of the heat-conduction type, *Adv. Comput. Math.*, *6*(1), 207–226, doi:10.1007/BF02127704.

Domine, F., and C. Rauzy (2004), Influence of the ice growth rate on the incorporation of gaseous HCl, *Atmos. Chem. Phys.*, *4*, 2513–2519, doi:10.5194/acp-4-2513-2004.

Domine, F., and P. B. Shepson (2002), Air-snow interactions and atmospheric chemistry, *Science*, *297*(5586), 1506–1510, doi:10.1126/science.1074610.

Domine, F., and E. Thibert (1996), Mechanism of incorporation of trace gases in ice grown from the gas phase, *Geophys. Res. Lett.*, *23*(24), 3627–3630, doi:10.1029/96GL03290.

Domine, F., E. Thibert, E. Silvente, M. Legrand, and J. L. Jaffrezo (1995), Determining past atmospheric HCl mixing ratios from ice core analyses, *J. Atmos. Chem.*, *21*(2), 165–186, doi:10.1007/BF00696579.

Domine, F., A. Cabanes, and L. Legagneux (2002), Structure, microphysics, and surface area of the Arctic snowpack near Alert during the ALERT 2000 campaign, *Atmos. Environ.*, *36*(15–16), 2753–2765, doi:10.1016/S1352-2310(02)00108-5.

Domine, F., A.-S. Taillandier, and W. R. Simpson (2007), A parameterization of the specific surface area of seasonal snow for field use and for models of snowpack evolution, *J. Geophys. Res.*, *112*, F02031, doi:10.1029/2006JF000512.

Domine, F., M. Albert, T. Huthwelker, H. W. Jacobi, A. A. Kokhanovsky, M. Lehning, G. Picard, and W. R. Simpson (2008), Snow physics as relevant to snow photochemistry, *Atmos. Chem. Phys.*, *8*, 171–208, doi:10.5194/acp-8-171-2008.

Domine, F., A. S. Taillandier, A. Cabanes, T. Douglas, and M. Sturm (2009), Three examples where the specific surface area of snow increased over time, *Cryosphere*, *3*(1), 31–39, doi:10.5194/tc-3-31-2009.

Döppenschmidt, A., and H. J. Butt (2000), Measuring the thickness of the liquid-like layer on ice surfaces with atomic force microscopy, *Langmuir*, *16*(16), 6709–6714, doi:10.1021/la990799w.

Ervens, B., P. Herckes, G. Feingold, T. Lee, J. L. Collett, and S. M. Kreidenweis (2003), On the drop-size dependence of organic acid and formaldehyde concentrations in fog, *J. Atmos. Chem.*, *46*(3), 239–269, doi:10.1023/A:1026393805907.

Evans, M. J., et al. (2003), Coupled evolution of BrO_x-ClO_x-HO_x-NO_x chemistry during bromine-catalyzed ozone depletion events in the arctic boundary layer, *J. Geophys. Res.*, *108*(D4), 8368, doi:10.1029/2002JD002732.

Gallet, J. C., F. Domine, C. S. Zender, and G. Picard (2009), Measurement of the specific surface area of snow using infrared reflectance in an integrating sphere at 1310 and 1550 nm, *Cryosphere*, *3*(2), 167–182, doi:10.5194/tc-3-167-2009.

Grannas, A. M., et al. (2002), A study of photochemical and physical processes affecting carbonyl compounds in the Arctic atmospheric boundary layer, *Atmos. Environ.*, *36*(15–16), 2733–2742, doi:10.1016/S1352-2310(02)00134-6.

Grannas, A. M., et al. (2007), An overview of snow photochemistry: Evidence, mechanisms and impacts, *Atmos. Chem. Phys.*, *7*, 4329–4373, doi:10.5194/acp-7-4329-2007.

Guimbaud, C., et al. (2002), Snowpack processing of acetaldehyde and acetone in the Arctic atmospheric boundary layer, *Atmos. Environ.*, *36*(15–16), 2743–2752, doi:10.1016/S1352-2310(02)00107-3.

Hantal, G., P. Jedlovszky, P. N. M. Hoang, and S. Picaud (2007), Calculation of the adsorption isotherm of formaldehyde on ice by grand canonical Monte Carlo simulation, *J. Phys. Chem. C*, *111*(38), 14,170–14,178, doi:10.1021/jp0742564.

Houdier, S., S. Perrier, E. Defrancq, and M. Legrand (2000), A new fluorescent probe for sensitive detection of carbonyl compounds: Sensitivity improvement and application to environmental water samples, *Anal. Chim. Acta*, *412*(1–2), 221–233, doi:10.1016/S0003-2670(99)00875-2.

Houdier, S., S. Perrier, F. Domine, A. Cabanes, L. Legagneux, A. M. Grannas, C. Guimbaud, P. B. Shepson, H. Boudries, and J. W. Bottenheim (2002), Acetaldehyde and acetone in the Arctic snowpack during the ALERT2000 campaign: Snowpack composition, incorporation processes and atmospheric impact, *Atmos. Environ.*, *36*(15–16), 2609–2618, doi:10.1016/S1352-2310(02)00109-7.

Houdier, S., M. Barret, F. Domine, T. Charbouillot, L. Deguillaume, and D. Voisin (2011), Sensitive determination of glyoxal, methylglyoxal and hydroxyacetaldehyde in environmental water samples by using Dansylacetamidooxyamine derivatization and liquid chromatography/fluorescence, *Anal. Chim. Acta*, doi:10.1016/j.aca.2011.08.022, in press.

Hutterli, M. A., R. Röthlisberger, and R. C. Bales (1999), Atmosphere-to-snow-to-firn transfer studies of HCHO at Summit, Greenland, *Geophys. Res. Lett.*, *26*(12), 1691–1694, doi:10.1029/1999GL900327.

Hutterli, M. A., R. C. Bales, J. R. McConnell, and R. W. Stewart (2002), HCHO in Antarctic snow: Preservation in ice cores and air-snow exchange, *Geophys. Res. Lett.*, *29*(8), 1235, doi:10.1029/2001GL014256.

Hutterli, M. A., J. R. McConnell, R. C. Bales, and R. W. Stewart (2003), Sensitivity of hydrogen peroxide (H_2O_2) and formaldehyde (HCHO) preservation in snow to changing environmental conditions: Implications for ice core records, *J. Geophys. Res.*, *108*(D1), 4023, doi:10.1029/2002JD002528.

Legagneux, L., A. Cabanes, and F. Domine (2002), Measurement of the specific surface area of 176 snow samples using methane adsorption at 77 K, *J. Geophys. Res.*, *107*(D17), 4335, doi:10.1029/2001JD001016.

Matsumoto, K., S. Kawai, and M. Igawa (2005), Dominant factors controlling concentrations of aldehydes in rain, fog, dew water, and in the gas phase, *Atmos. Environ.*, *39*(38), 7321–7329, doi:10.1016/j.atmosenv.2005.09.009.

McConnell, J. R., R. C. Bales, R. W. Stewart, A. M. Thompson, M. R. Albert, and R. Ramos (1998), Physically based modeling of atmosphere-to-snow-to-firn transfer of H_2O_2 at South Pole, *J. Geophys. Res.*, *103*(D9), 10,561–10,570, doi:10.1029/98JD00460.

Odabasi, M., and R. Seyfioglu (2005), Phase partitioning of atmospheric formaldehyde in a suburban atmosphere, *Atmos. Environ.*, *39*(28), 5149–5156, doi:10.1016/j.atmosenv.2005.05.006.

Østerby, O. (2003), Five ways of reducing the Crank-Nicolson oscillations, *BIT Numer. Math.*, *43*(4), 811–822, doi:10.1023/B:BITN.0000009942.00540.94.

Perrier, S., S. Houdier, F. Domine, A. Cabanes, L. Legagneux, A. L. Sumner, and P. B. Shepson (2002), Formaldehyde in Arctic snow: Incorporation into ice particles and evolution in the snowpack, *Atmos. Environ.*, *36*(15–16), 2695–2705, doi:10.1016/S1352-2310(02)00110-3.

Perrier, S., P. Sassin, and F. Domine (2003), Diffusion and solubility of HCHO in ice: Preliminary results, *Can. J. Phys.*, *81*(1–2), 319–324, doi:10.1139/p03-033.

Pomeroy, J. W., and L. Li (2000), Prairie and arctic areal snow cover mass balance using a blowing snow model, *J. Geophys. Res.*, *105*(D21), 26,619–26,634, doi:10.1029/2000JD900149.

Pomeroy, J. W., D. M. Gray, and P. G. Landine (1993), The Prairie Blowing Snow Model: Characteristics, validation, operation, *J. Hydrol.*, *144*(1–4), 165–192, doi:10.1016/0022-1694(93)90171-5.

Shepson, P. B., A.-P. Sirju, J. F. Hopper, L. A. Barrie, V. Young, H. Niki, and H. Dryfhout (1996), Sources and sinks of carbonyl compounds in the Arctic Ocean boundary layer: Polar ice floe experiment, *J. Geophys. Res.*, *101*(D15), 21,081–21,089, doi:10.1029/96JD02032.

Sumner, A. L., and P. B. Shepson (1999), Snowpack production of formaldehyde and its effect on the Arctic troposphere, *Nature*, *398*(6724), 230–233, doi:10.1038/18423.

Sumner, A. L., et al. (2002), Atmospheric chemistry of formaldehyde in the Arctic troposphere at polar sunrise, and the influence of the snowpack, *Atmos. Environ.*, *36*(15–16), 2553–2562, doi:10.1016/S1352-2310(02)00105-X.

Thibert, E., and F. Domine (1997), Thermodynamics and kinetics of the solid solution of HCl in ice, *J. Phys. Chem. B*, *101*(18), 3554–3565, doi:10.1021/jp962115o.

Thibert, E., and F. Domine (1998), Thermodynamics and kinetics of the solid solution of HNO_3 in ice, *J. Phys. Chem. B*, *102*(22), 4432–4439, doi:10.1021/jp980569a.

Walden, V. P., S. G. Warren, and E. Tuttle (2003), Atmospheric ice crystals over the Antarctic Plateau in winter, *J. Appl. Meteorol.*, *42*(10), 1391–1405, doi:10.1175/1520-0450(2003)042<1391:AICOTA>2.0.CO;2.

Weibring, P., D. Richter, J. G. Walega, and A. Fried (2007), First demonstration of a high performance difference frequency spectrometer on airborne platforms, *Opt. Express*, *15*(21), 13,476–13,495, doi:10.1364/OE.15.013476.

Weibring, P., D. Richter, J. G. Walega, L. Rippe, and A. Fried (2010), Difference frequency generation spectrometer for simultaneous multi-species detection, *Opt. Express*, *18*(26), 27,670–27,681, doi:10.1364/OE.18.027670.

Winkler, A. K., N. S. Holmes, and J. N. Crowley (2002), Interaction of methanol, acetone and formaldehyde with ice surfaces between 198 and 223 K, *Phys. Chem. Chem. Phys.*, *4*(21), 5270–5275, doi:10.1039/b206258e.

M. Barret, F. Domine, J.-C. Gallet, and S. Houdier, Laboratoire de Glaciologie et Géophysique de l'Environnement, CNRS and Université Joseph Fourier – Grenoble I, BP 96, F-38402 Saint-Martin-d'Hères CEDEX, France. (florent@lgge.obs.ujf-grenoble.fr)

A. Fried, D. Richter, J. Walega, and P. Weibring, Earth Observing Laboratory, National Center for Atmospheric Research, 3450 Mitchell Lane, Boulder, CO 80301, USA.